

Clusters of Galaxies in the SDSS

R. C. Nichol
Dept. of Physics, Carnegie Mellon University

Abstract

I review here past and present research on clusters and groups of galaxies within the Sloan Digital Sky Survey (SDSS). I begin with a short review of the SDSS and efforts to find clusters of galaxies using both the photometric and spectroscopic SDSS data. In particular, I discuss the C4 algorithm which is designed to search for clusters and groups within a 7-dimensional data-space, *i.e.*, simultaneous clustering in both color and space. Also, the C4 catalog has a well quantified selection function based on mock SDSS galaxy catalogs constructed from the Hubble Volume simulation. The C4 catalog is $> 90\%$ complete, with $< 10\%$ contamination, for halos of $M_{200} > 10^{14} M_{\odot}$ at $z < 0.14$. Furthermore, the observed summed r -band luminosity of C4 clusters is linearly related to M_{200} with $< 30\%$ scatter at any given halo mass. I also briefly review the selection and observation of Luminous Red Galaxies (LRGs) and demonstrate that these galaxies have a similar clustering strength as clusters and groups of galaxies. I outline a new collaboration planning to obtain redshifts for 10,000 LRGs at $0.4 < z < 0.7$ using the SDSS photometric data and the AAT 2dF instrument. Finally, I review the role of clusters and groups of galaxies in the study of galaxy properties as a function of environment. In particular, I discuss the “SFR–Density” and “Morphology–Radius” relations for the SDSS and note that both of these relationships have a *critical density* (or “break”) at a projected local galaxy density of $\simeq 1 h_7^2 \text{Mpc}^{-2}$ (or between 1 to 2 virial radii). One possible physical mechanism to explain this observed critical density is the stripping of warm gas from the halos of in-falling spiral galaxies, thus leading to a slow strangulation of star-formation in these galaxies. This scenario is consistent with the recent discovery (within the SDSS) of an excess of “Passive” or “Anemic” spiral galaxies located within the in-fall regions of C4 clusters.

1.1 Introduction

As demonstrated by this conference – *Clusters of Galaxies: Probes of Cosmological Structure and Galaxy Evolution* –, clusters and groups of galaxies have a long history as key tracers of the large-scale structure in the Universe and as laboratories within which to study the physics of galaxy evolution. At the conference, their important role as cosmological probes was reviewed by several speakers, including Simon White, Alan Dressler, Gus Oemler and Guinevere Kauffmann. Therefore, I will not dwell on justifying the importance

R. C. Nichol

of clusters to cosmological research, but simply direct the reader to the reviews by these authors.

Instead, I provide below a brief overview of the Sloan Digital Sky Survey (SDSS), followed by a discussion of the cluster-finding algorithms (Section 1.2) used within the SDSS collaboration and present new scientific results obtained from studies of galaxies as a function of environment (Section 1.5).

1.1.1 The Sloan Digital Sky Survey

The Sloan Digital Sky Survey (SDSS; York et al. 2000; Stoughton et al. 2002) is a joint multi-color (u, g, r, i, z) imaging and medium resolution ($R=1800$; 3700\AA to 9100\AA) spectroscopic survey of the northern hemisphere using a dedicated 2.5 meter telescope located at the Apache Point Observatory near Sunspot in New Mexico. During well-defined (seeing $< 1.7''$) photometric conditions, the SDSS employs a mosaic camera of 54 CCD chips to image the sky via the drift-scanning technique (see Gunn et al. 1998). These data are reduced at Fermilab using a dedicated photometric analysis pipeline (PHOTO; see Lupton et al. 2001) and object catalogs obtained for spectroscopic target selection. During non-photometric conditions, the SDSS performs multi-object spectroscopy using two bench spectrographs attached to the SDSS telescope and fed with 640 optical fibers. The other ends of these fibers are plugged into a pre-drilled aluminum plate that is bent to follow the 3-degree focal surface of the SDSS telescope. The reader is referred to Smith et al. (2002), Blanton et al. (2003) and Pier et al. (2003) for more details about the SDSS.

In this way, the SDSS plans to image the northern sky in 5-passbands as well as obtaining spectra for $\sim 10^6$ objects. In addition to the large amount of the data being collected, the quality of the SDSS data is high, which is important for many of the scientific goals of the survey. For example, the SDSS has a dedicated Photometric Telescope (PT; Hogg et al. 2001) which is designed to provide the SDSS with a global photometric calibration of a few percent over the whole imaging survey. Also, SDSS spectra are spectrophotometrically calibrated.

The SDSS is now in production mode and has been collecting data for several years. As of January 2003, the SDSS had obtained 4470 deg^2 of imaging data (not unique area) and had measured a half million spectra. The SDSS has just announced its first official data release (see <http://www.sdss.org/dr1/>).

1.2 SDSS Cluster Catalogs

One of the fundamental science goals of the SDSS was to create new catalogs of clusters from both the imaging and spectroscopic data. In Table 1.1, I present a brief overview of past and present efforts within the SDSS collaboration as part of the SDSS Cluster Working Group. In this table, I provide an appropriate reference if available, a brief description of the cluster-finding algorithm and the SDSS data being used to find clusters. Each of these algorithms have different strengths and science goals, and a detailed knowledge of their selection functions is required before a fair comparison can be carried out between these different catalogs. The reader is referred to the review of Postman (2002) for more discussion of this point. However, Bahcall et al. (2003) has begun this process by performing a detailed comparison of the clusters found by both the AMF and maxBCG

Table 1.1. Overview of past and present efforts to find clusters and groups of galaxies within the SDSS collaboration. In the data column, “I” is for SDSS imaging data and “S” is for SDSS spectral data.

Name	Reference	Data	Description
maxBCG	Annis et al.	I	Model colors of BCG with z and look for E/S0 ridge-line
AMF	Kim et al. (2002)	I	Matched Filter algorithm looking for over-densities in luminosity & space
CE	Goto et al. (2002)	I	Color-cuts, then uses Sextractor to find and de-blend clusters
F-O-F	Berlind et al.	S	Friends-of-friends algorithm
Groups	Lee et al. (2003)	I	Mimics Hicksons Groups criteria
BH	Bahcall et al. (2003)	I	Merger of maxBCG & AMF
C4	Nichol et al. (2001)	I & S	Simultaneous clustering of galaxies in color & space

algorithms. The product of this work is a joint catalog of 799 clusters in the redshift range $0.05 < z_{est} < 0.3$ selected from $\sim 400\text{deg}^2$ of early SDSS commissioning data.

As first outlined in Nichol (2001), there are main four challenges to producing a robust optically-selected catalog of clusters. These are:

- (1) To eliminate projection effects. This problem has plagued previous catalogs of clusters and has been discussed by many authors (see, for example, Lucey et al. 1983; Sutherland 1988; Nichol et al. 1992; Postman et al. 1992; Miller 2000);
- (2) A full understanding of the selection function. This has been traditionally ignored for optical cluster catalogs (see Bramel et al. 2000; Kochanek et al. 2003), but is critical for all statistical analyzes using the catalog;
- (3) To provide a robust mass estimator. Traditionally, this has been the Achilles’ Heel of optical catalogs, as richness is a poor indicator of mass; and,
- (4) To cover a large dynamic range in both redshift and mass

I review below one SDSS cluster catalog I am involved with, in collaboration with Chris Miller at CMU, that now meets these four challenges and is comparable in quality to the best X-ray catalogs of clusters (*e.g.*, the REFLEX catalog of Böhringer et al. 2001).

1.3 The C4 Algorithm

The underlying hypothesis of the C4 algorithm is that a cluster or group of galaxies is a clustering of galaxies in both color and space. This is demonstrated in Figure 1.1 and the reader is referred to Gladders & Yee (2000) for a full discuss of all the evidence in support of this hypothesis. Therefore, by searching for clusters simultaneously in both color and space, the C4 algorithm reduces projection effects to almost zero, while still retaining much power for finding clusters (see Figure 1.2).

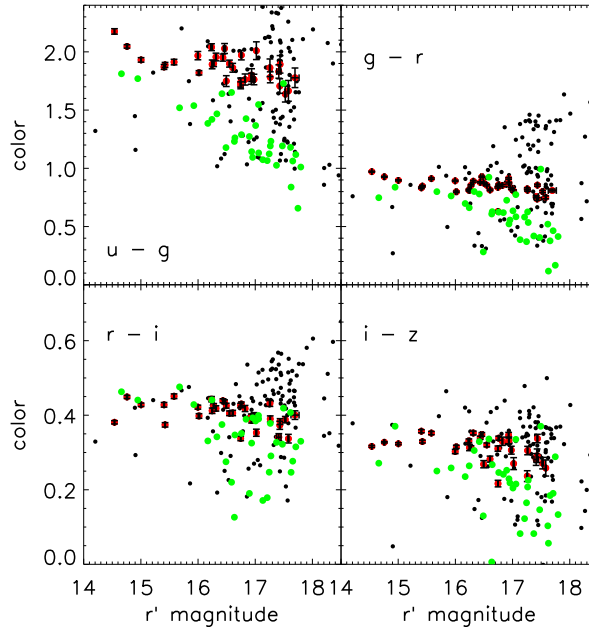


Fig. 1.1. The color-magnitude relations for a previously undiscovered $z=0.06$ cluster in the Early Data Release of the SDSS detected by the C4 algorithm. The black dots are galaxies within an aperture of $1h^{-1}\text{Mpc}$ around the cluster center. The red and green dots are actual cluster members (within $4\sigma_r$ in redshift space). The red points are galaxies with a low H_α equivalent width, while green points are galaxies with a high H_α equivalent width, *i.e.*, passive and star-forming galaxies respectively. The errors on the colors are shown for the red points, indicating the typical error bars on colors within the SDSS spectroscopic sample. Note the tight correlation in color of the red points, which is the E/S0 ridge line and is the signal the C4 algorithm is using to find clusters.

1.3.1 Overview of C4 Algorithm

I present here a brief overview of the C4 algorithm. To date, the C4 algorithm has been applied to the SDSS main galaxy spectroscopic sample (Strauss et al. 2002) in the Early Data Release (EDR) of the SDSS (see Stoughton et al. 2002; Gómez et al. 2003).

For each galaxy in the sample – called the “target” galaxy below – the C4 algorithm is performed in the following steps:

- (1) A 7-dimensional square box is placed on the target galaxy. The center of this box is defined by the observed photometric colors (*i.e.*, $u-g$, $g-r$, $r-i$, $i-z$), the Right Ascension, Declination and redshift of the target galaxy. The width of the box is dependent on the redshift and photometric errors on the colors of the target galaxy. Once the box is defined, the number of neighboring galaxies is counted within the SDSS main galaxy sample (Strauss et al. 2002) inside this box and this count is reported (see Figure 1.2).
- (2) The same 7-D box is placed on 100 randomly chosen galaxies, also taken from the SDSS main galaxy spectroscopic sample, that possess similar seeing and reddening values (see

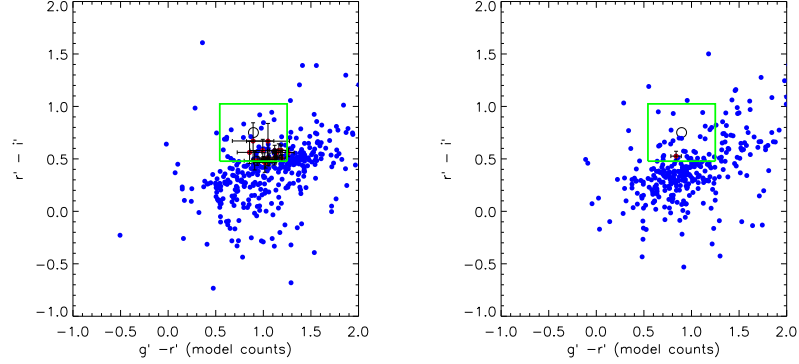


Fig. 1.2. Color-color plots for an example cluster galaxy (left) and one randomly chosen field position (right). The blue dots are all galaxies within the spatial part of the 7–dimensional search box centered on the target galaxy (*i.e.*, all galaxies satisfying the RA, Dec, and z dimensions of the 7D box). The red points are now those galaxies which also lie within the color part of the 7–dimensional search box, *i.e.*, they are close in both space and color. The size of the 7D box in this color-color plane is shown in green. As you can see it is much smaller than the scatter seen in the blue points (close in just the spatial coordinates). For the random field position (right), there is only one red point inside the box compared to ten around the cluster galaxy (left). Therefore, all projection effects have been eradicated as one does not expect false clustering in such a high dimensional space.

Figure 1.2). For each of these 100 randomly chosen galaxies, the number of neighboring galaxies is counted (from the SDSS main galaxy sample) inside the box and a distribution of galaxy counts is constructed from these 100 randomly chosen galaxies.

- (3) Using this observed distribution of galaxy counts, the probability of obtaining the observed galaxy count around the original target galaxy is computed.
- (4) This exercise is repeated for all galaxies in the sample and then rank all these probabilities.
- (5) Using FDR (Miller et al. 2001) with an $\alpha = 0.2$ (*i.e.*, only allowing a false discovery rate of 20%), a threshold in probability is determined that corresponds to galaxies that possess a high count of nearest neighbors in their 7–dimensional box.
- (6) All galaxies in our sample below this threshold in probability are removed, which results in the eradication $\simeq 80\%$ of all galaxies. By design, the galaxies that are removed are preferentially in low density regions of this 7–dimensional space (*i.e.*, the field population). The galaxies that remain are called “C4 galaxies” which, by design, reside in high density regions with neighboring galaxies that possess the same colors as the target galaxy. Figure 1.3 illustrates this step
- (7) Using only the C4 galaxies, the local density of all the C4 galaxies is determined using the distance to the 8th nearest neighbor.
- (8) The galaxies are rank order based on these measured densities and then assigned to clusters based on this ranked list. This is the same methodology as used to create halo catalogs within N–body simulations (see Evrard et al. 2002).
- (9) This results in a list of clusters, for which a summed total optical luminosity (z and r bands) and a velocity dispersion are computed (see below).

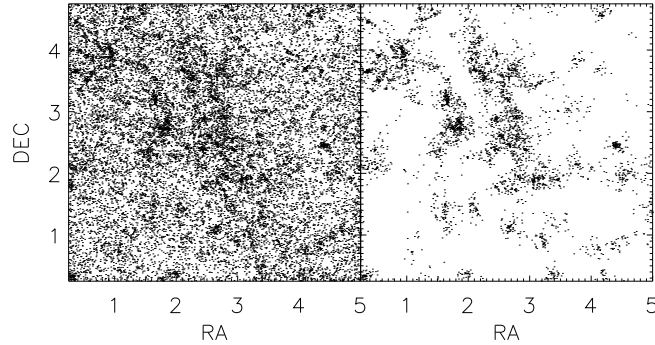


Fig. 1.3. The projected galaxy distribution in the simulations before (left) and after (right) the C4 algorithm have been run and a threshold applied to eliminate field-like galaxies. This illustrates the effect of Step 6 in the algorithm.

In summary, the C4 algorithm is a semi-parametric implementation of adaptive kernel density estimation. The key difference with this approach, compared to previous cluster-finding algorithms, is that it does not model either the colors of cluster ellipticals (*e.g.*, Gladders & Yee 2000, Goto et al. 2003), or the properties of the clusters (*e.g.*, Postman et al. 1996; Kepner et al. 1999; Kim et al. 2002). Instead, the C4 algorithm only demands that the colors of nearby galaxies are the same as the target galaxy. In this way, the C4 algorithm is sensitive to a diverse range of clusters and groups, *e.g.*, it would detect a cluster dominated by a extremely “blue” population of galaxies (compared to the colors of field galaxies). Therefore, the C4 catalog can be used for studying galaxy evolution in clusters with little fear that the sample is biased against certain types of systems.

1.3.2 Simulations of the SDSS Data

To address the four challenges given above, it is vital that we construct realistic simulations of the C4 cluster catalog. This has now been achieved through collaboration with Risa Wechsler, Gus Evrard and Tim McKay at the University of Michigan. Briefly, mock SDSS galaxy catalogs have been created using the dark matter distribution from the Hubble Volume simulations (Evrard et al 2002)*. The procedure for populating the dark matter distribution with galaxies is described by Wechsler in this proceedings, and in further detail by Wechsler et al (in preparation), but I present a brief overview here. The simulation we use provides the dark matter distribution of the full sky out to $z \sim 0.6$, where the dark matter clustering is computed on a light cone. Galaxies, with r-band luminosities following the luminosity function found by Blanton et al (2001) for the SDSS, are added to the simulation by choosing simulation particles (with mass $\simeq 2.2 \times 10^{12} M_{\odot}$ per particle) from a probability density function (PDF) of local mass density which depends on galaxy luminosity. This luminosity dependent PDF is tuned so that the resulting galaxies match the luminosity dependent 2-point correlation function (Zehavi et al. 2002). Colors are then added to the simulation using the colors of actual SDSS galaxies with similar luminosities

* <http://www.mpa-garching.mpg.de/Virgo/hubble.html>

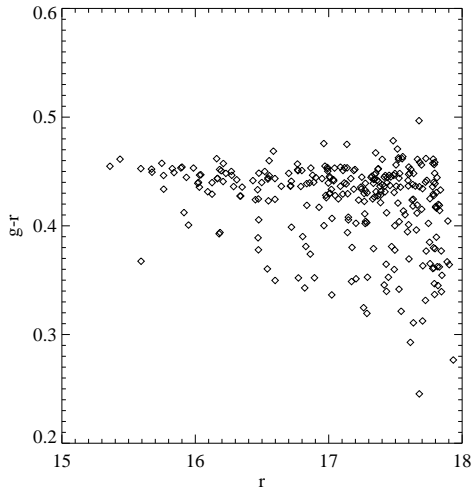


Fig. 1.4. The color–magnitude relation for a $10^{15}M_{\odot}$ halo in the Hubble Volume simulation, where galaxies with SDSS colors and luminosities have been added to the simulation using the prescription outlined by Wechsler in this proceedings.

and local galaxy densities. The resulting catalog thus matches the luminosity function and color- and luminosity-dependent 2-point correlation function of the SDSS data.

Therefore, these mock SDSS catalogs produce clusters of galaxies with a realistic color–magnitude diagram (compare Figures 1.1 and 1.4). As we know the location of all the massive halos (*i.e.*, the clusters) within the Hubble Volume simulation (see Jenkins et al. 2000 & Evrard et al. 2002), we can now use these mock catalogs to derive the selection function of the C4 algorithm. The benefit of this approach is that these mock catalogs contain realistic projection effects, as the galaxy clustering is constrained to match the real data, and the clusters (halos) possess realistic profiles, ellipticities and morphologies. This is a significant advancement on past simulations used to quantify the selection function of cluster catalogs (see Bramel et al. 2000; Postman et al. 1996; Goto et al. 2002).

For comparison between the real and simulated data, two different cluster observables are used. The first is the bi-weighted velocity dispersion and the second is the summed optical luminosity of the galaxies within the cluster. To calculate the velocity dispersion (σ_v), an iterative technique is performed using the robust bi-weighted statistics of Beers et al. (1990). The total optical luminosity of the clusters is determined by converting the apparent magnitudes of galaxies in the cluster to optical luminosities using the conversions in Fukugita et al. (1996). All magnitudes are also k -corrected according to Blanton et al. (2002) and extinction corrected according to Schlegel, Finkbeiner, and Davis (1998). Cluster membership is defined to be any galaxy within $4\sigma_v$ in redshift, and within $1.5h^{-1}Mpc$ projected separation on the sky. For the halo catalog, the mass within 200 times the critical density (M_{200}) is used as determined from summing up all the dark matter particles within this radius around each halo (R_{200} ; see Evrard et al. 2002).

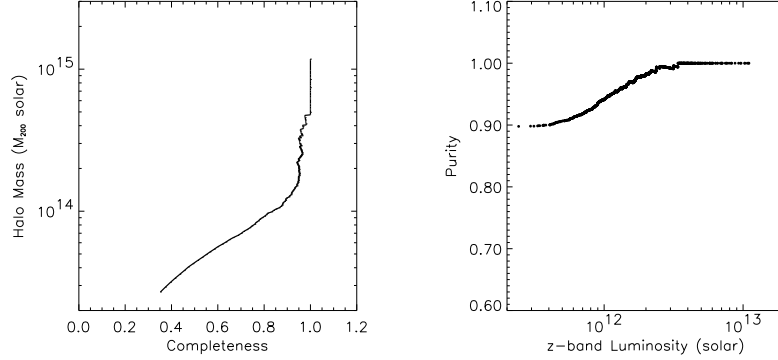


Fig. 1.5. (Left) The completeness of the C4 catalog as a function of the dark matter halo mass from the simulation (M_{200}). (Right) The purity of the C4 catalog, as a function of the summed total r -band luminosity of the cluster, as derived from our mock SDSS galaxy catalog.

1.3.3 Purity and Completeness: Challenges One and Two

The C4 algorithm has been applied to these mock SDSS galaxy catalogs. In Figure 1.5, I show the purity of the matched C4 clusters found in the simulation as a function of the total r band luminosity. Purity is defined to be the percentage of systems detected in the mock SDSS catalog, using the C4 algorithm, that match a known dark matter halo in the HV simulation. Clearly, the purity of the C4 catalog remains high over nearly 2 orders of magnitude in luminosity and is a direct result of searching for clustering in a high-dimensional space where projection effects are rare.

In Figure 1.5, I also present the completeness of the C4 catalog, as a function of the dark halo mass (M_{200}), and demonstrate that the C4 catalog remains $> 90\%$ complete for systems with $M_{200} > 10^{14}M_{\odot}$. The accuracy of these completeness measurements greatly benefits from the large sample sizes available from the HV simulation. However, for the lower mass systems, there may be some incompleteness in the original dark matter halo catalog because of the mass resolution of the HV simulations. Furthermore, the purity and completeness of the C4 catalog is only a weak function of the input parameters, *e.g.*, the FDR threshold, and thus robust against the exact parameter choices. In summary, using these mock SDSS catalogs, we have addressed the first two challenges given in Section 1.2, *i.e.*, for $z < 0.14$, the C4 catalog is $> 90\%$ complete, with $< 10\%$ contamination, for halos of $M_{200} > 10^{14}M_{\odot}$.

1.3.4 Mass Estimator and Dynamic Range: Challenges Three and Four

In Figure 1.6, I present the correlation between the M_{200} dark matter halo mass (taken directly from Evrard et al. 2002) and the total summed r band luminosities for 4734 clusters that match in the HV simulation. As expected, these two quantities are linearly correlated over 2 orders of magnitude in both the halo mass and optical luminosity. The measured scatter for the whole dataset is 25% (measured perpendicular to the best fit line). This plot demonstrates that we have address the 3rd and 4th challenges in Section 1.2.

In the future, the C4 algorithm will be extended to include: *i)* Higher resolution dark

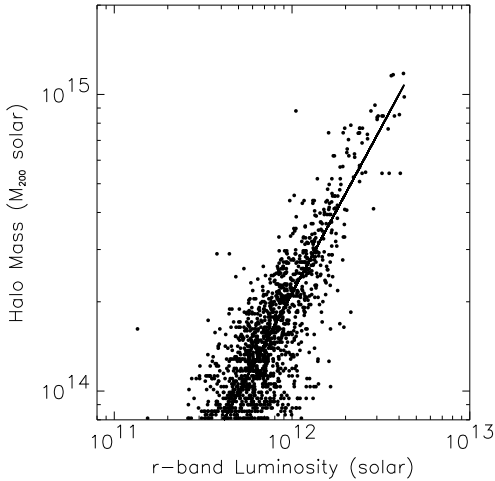


Fig. 1.6. The relation between the dark matter halo mass in our simulation and the total summed r luminosity. The line is the best fit and the scatter, for a given mass, is $< 30\%$.

matter simulations to test the sensitivity of the algorithm to lower mass systems; *ii*) A range of cosmological simulations to probe our sensitivity to various cosmological parameters *e.g.*, σ_8 ; and *iii*) Improve our methods of populating the simulations with SDSS galaxies using higher order statistics (*e.g.*, the 3–point correlation function).

1.4 Luminous Red Galaxies

I briefly review here forthcoming surveys of Luminous Red Galaxies (LRGs) as these surveys will soon replace clusters as the most efficient tracers of the large–scale structure in the Universe. Such galaxies are selected to be dominated by an old stellar population (using the SDSS colors) and are luminous, so they can be seen to high redshift even in the SDSS photometric data (see Eisenstein et al. 2001 for details).

A preliminary analysis of the correlation functions for both a sample of LRGs, selected from the SDSS (Eisenstein et al. 2001), and normal SDSS galaxies (Zehavi et al. 2001), demonstrates that, as expected, the LRGs are more strongly clustered than normal galaxies. The LRG correlation function has an amplitude and scale–length consistent with that measured for groups and clusters of galaxies (*e.g.*, Peacock & Nicholson 1991; Nichol et al. 1992; Collins et al. 2000; Miller 2000; Nichol 2002). Therefore, by design, a large fraction of these LRGs must lie in dense environments as their spatial distribution clearly traces the distribution of clusters and groups in the universe. The main advantage of the LRG selection is that it does not depend upon the details of finding clusters of galaxies, and therefore, their selection is more straightforward to model (see Eisenstein et al. 2001).

Due to the 45 minute spectroscopic exposure time of the SDSS, the SDSS only targets LRG candidates brighter than $r = 19.5$ (Eisenstein et al. 2001). This corresponds to a cut–off at $z \simeq 0.45$, but one can easily detect LRG candidates in the SDSS photometric data to

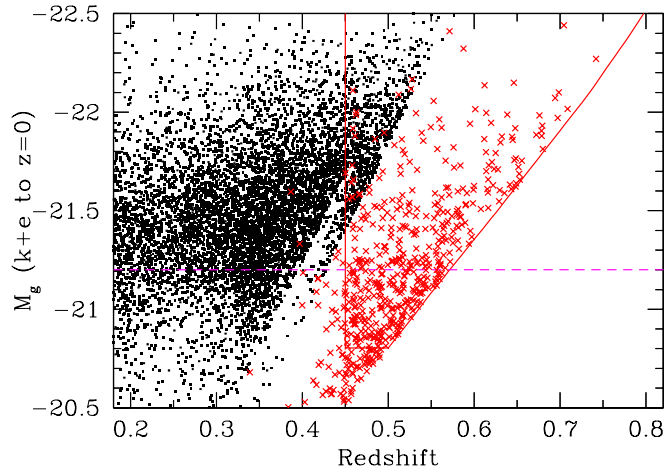


Fig. 1.7. The distribution in g-band luminosity and redshift for both the low redshift LRGs (solid points) and the SDSS-2dF LRGs (red crosses). The luminosities are k-corrected and corrected for passive evolution to $z = 0$. The red lines show the expected selection boundaries for the SDSS-2dF survey, while the dashed line is the luminosity limit above which we expect the low redshift SDSS LRG sample to be complete. Plot courtesy of Daniel Eisenstein and my SDSS-2dF colleagues.

higher redshifts*. Therefore, using the unique 2dF multi-object spectrograph on the Anglo-Australian Telescope, we have begun a joint SDSS-2dF program to push the original SDSS LRG selection to higher redshift. At the time of writing, our initial observations have been very successful, with spectra for $\simeq 1000$ LRGs in the redshift range of $0.4 < z < 0.7$. In Figure 1.7, I show the distribution in luminosity and redshift of these new SDSS-2dF LRGs and highlight that they cover a comparable range in their luminosities as the low redshift LRGs. By the end of the SDSS-2dF LRG survey, we hope to have redshifts for 10,000 LRGs over this intermediate redshifts range. When combined with the low redshift SDSS LRGs, we will be able to study the evolution in the properties and clustering of a single population of massive galaxies over half the age of the universe.

1.5 Galaxy Properties as a Function of Environment

Clusters and groups of galaxies play an important role in studying the effects of environment on the properties of galaxies. With the SDSS data, it is now possible to extend such studies well beyond the cores of clusters into lower density environments. Furthermore, the distance to the N^{th} nearest neighbor can be used to provide an adaptive measure of the local density of galaxies (see Dressler et al. 1980; Lewis et al. 2002; Gómez et al. 2003). One can also use kernel density estimators (*e.g.*, Eisenstein 2003) and mark correlation functions.

There were many great talks and posters on the topic of galaxy evolution in clusters at this conference. For example, see the contributions by Bower, Davis, Dressler, Franx, Goto,

* Beyond $z=0.45$, the SDSS LRG selection becomes easier than at lower redshift (with less contamination) because of the fortuitous design of the SDSS filter system, see Eisenstein et al. (2001)

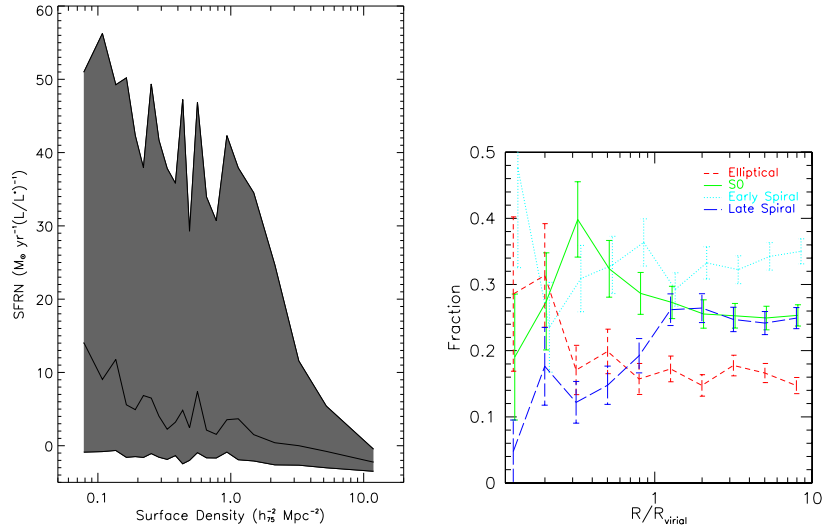


Fig. 1.8. (Left) The relation between SFR and density for a volume–limited sample of 8598 SDSS galaxies between $0.05 < z < 0.095$. The y–axis is the normalized SFR, *i.e.*, the SFR divided by the z luminosity of the galaxy. The x–axis is the projected local surface density computed from the distance to the 10th nearest neighbor in a redshift shell of $\pm 1000 \text{ km s}^{-1}$. See Gómez et al. (2003) for details. The top of the shaded region is the 75th percentile of the distribution, while the bottom is the 25th percentile. The solid line through the shaded area is the median of the distribution. As one can see, beyond a density of $\simeq 1 h_{75}^2 \text{ Mpc}^{-2}$, the tail of the distribution (75th percentile) is heavily curtailed in dense environments. (Right) The morphology–radius relation for C4 clusters in the SDSS. The morphologies were derived using the T_{auto} parameter discussed in the text, while the distance to the nearest C4 cluster (y–axis) has been scaled by the virial radius of that clusters. These plots were taken from Gómez et al. (2003) and Goto et al. (in prep).

Koo, Kauffmann, Martini, N. & C. Miller, Postman, Poggianti, Tran and Treu. Also, I refer the reader to the work of Hogg et al. (2003) who is also using the SDSS data to study the effects of environment on the colors, surface brightnesses, morphologies and luminosities of galaxies.

1.5.1 Critical Density

Is the star–formation rate (SFR) of a galaxy affected by its environment? The answer appears to be yes, and was discussed by several authors at this conference (see the contributions by Miller, Couch and Bower). In particular, Gómez et al. (2003) find that the fraction of strongly star–forming galaxies in the SDSS decreases rapidly beyond a critical density of $\simeq 1 h_{75}^2 \text{ Mpc}^{-2}$ (see also Lewis et al. 2002). This result is demonstrated in Figure 1.8 and appears to be the same for all morphological types (see Gómez et al. 2003 and below).

In Figure 1.8, we also show a preliminary SDSS *Morphology–Radius* (T – R) relation based on the work of Goto et al. (in prep). The morphological classifications used in this figure are based on new, and improved, concentration index (C_m ; see Shimasaku et al. 2001)

R. C. Nichol

measurement of Yamauchi et al. (in prep). Briefly, Yamauchi et al. (in prep) compute their concentration index within two-dimensional, elliptical isotopes, which account for the observed ellipticity and orientation of the galaxy on the sky. This improvement helps prevent low inclination galaxies (*e.g.*, edge-on spirals) from being mis-classified as early-type galaxies. Furthermore, Yamauchi et al. (in prep) computes the “coarseness” of each galaxy, which is a measure of the residual variance after the best fit 2-D galaxy model has been subtracted. This coarseness measurement can therefore detect the presence of spiral arms in a galaxy. These two measurements of the morphology are re-normalized (by their rms) and added to produce a final morphological parameter called T_{auto} . Yamauchi et al. (in prep) has tested their algorithm extensively and have demonstrated that T_{auto} is more strongly correlated with visual morphological classifications than the normal C_{in} parameter, with a correlation coefficient with the visual morphologies of 0.89.

Using the T_{auto} classification, Goto et al. (in prep) has separated SDSS galaxies into the four (traditional) morphological subsamples of ellipticals, lenticulars (S0's), early spirals (Sa, Sb galaxies) and late spirals (Sc and Irregulars). This is presented in Figure 1.8. Clearly, the mapping between the T_{auto} parameter and these visually-derived morphological classifications is not perfect, but such an analysis does allow for an easier comparison with previous measurements of the T -R and Morphology-Density (T - Σ) relations, and theoretical predictions of these relationships (see Benson et al. 2000).

The SDSS T -R relation shown in Figure 1.8 remains constant at > 2 virial radii from C4 clusters. As expected, this corresponds to low density regions ($< 1 h_{75}^2 \text{Mpc}^{-2}$) in our volume-limited sample. This observation is consistent with previous determinations of the T - Σ and T -R relations in that these functions are near constant at low densities (see Dressler et al 1980; Postman et al. 1984; Dressler et al. 1997; Treu et al. 2003). At a radius of $\simeq 1$ virial radius, we witness a change in the T -R relation, *i.e.*, we see a decrease in the fraction of late spiral galaxies (\sim Sc galaxies) with smaller cluster-centric radii. We also see some indication of a decrease in the early spirals. It is interesting to note that the critical density of $\simeq 1 h_{75}^2 \text{Mpc}^{-2}$ seen in the SFR-Density relation of Gómez et al. corresponds to a cluster-centric radius of between $\simeq 1$ to 2 virial radii. The key question is; Are these two phenomena just different manifestations of the same physical process which is transforming both the morphology and SFR of the galaxies at this critical density? I believe the jury is still out on this question (but see the contributions of Bower and Miller in these proceedings).

I note here that Postman & Geller (1984) also reported a critical density (or “break”) in their T - Σ relation at approximately the same density as seen in Figure 1.8, *i.e.*, $\simeq 3.5 h_{75}^3 \text{Mpc}^{-3}$. Therefore, this “break” (or critical density) seen in the T - Σ relation appears to be universal, as it has been seen in two separate studies, which are based on different selection criteria and analysis techniques.

1.6 Strangulation of Star-Formation

One possible physical model* for explaining the critical density seen at $\simeq 1 h_{75}^2 \text{Mpc}^{-2}$ (or > 1 virial radius) in the SFR-Density and T -R relations is the stripping of the warm gas in the outer halo of in-falling spiral galaxies, via tidal interactions with the cluster potential. This process removes the reservoir of hydrogen which replenishes the gas in the cold disk of the galaxy, and thus slowly strangles (or starves) the star-formation in the disk leading

* See the reviews of Bower, Mihos & Moore for a discussion of other physical mechanisms that can affect the properties of galaxies in clusters and groups of galaxies

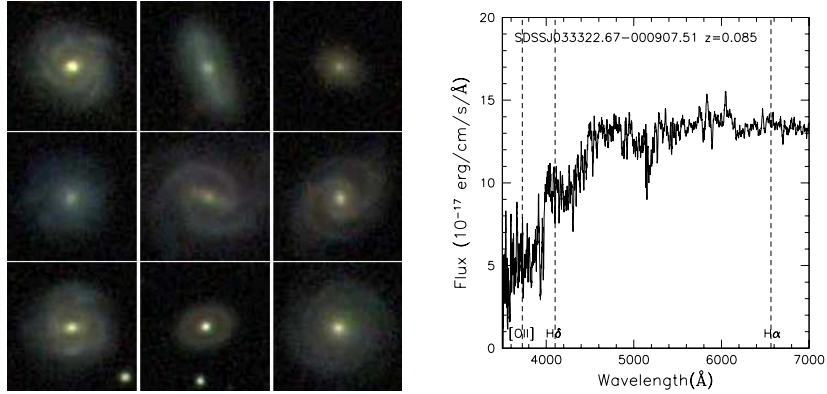


Fig. 1.9. (Left) Nine images of “Passive” spiral galaxies found by Goto et al. (2003) in their search for anemic galaxies in the SDSS database. Note the lack of “blue” HII star-forming regions in the arms of these spirals. (Right) The SDSS spectrum for one of these “Passive Spirals” (the galaxy in the top left-hand corner). Notice the lack of any emission lines indicative of on-going star-formation. This plot was taken from Goto et al. (2003).

to a slow death (see Larson et al. 1980; Diaferio et al. 2000; Balogh et al. 2000). Recent N-body simulations of this model by Bekki et al. (2002) demonstrate that it is a viable and can happen at large cluster radii (or low densities).

One possible observational consequence of this strangulation of star-formation is the existence of red, or passive, spiral galaxies, *i.e.*, galaxies that possess a spiral morphology, but have no observed on-going star-formation. Such galaxies have been found already in studies of high redshift clusters of galaxies (Couch et al. 1998) and have been known for sometime at low redshift as “Anemic Spirals” (see van den Bergh 1991), although their true nature has been debated by many (see Bothun & Sullivan 1980; Guiderdoni 1987 and the review of van Gorkom in these proceedings). Goto et al. (2003) has performed an automated search for such “Passive” or “Anemic” spirals within the SDSS database by looking for galaxies with a high C_{in} value (indicating a face-on spiral galaxy; see Shimasaku et al. 2001) but with no detected emission lines in their SDSS spectra. In total, they found 73 such galaxies, which comprises of only $0.28 \pm 0.03\%$ of all spiral galaxies with the same C_{in} parameter values, but with detected emission lines. I show some examples of these “Passive Spirals” in Figure 1.9.

The most interesting discovery of Goto et al. is the distribution of local densities for these “Passive Spirals”, which peaks at $\simeq 1h_7^2 \text{Mpc}^{-2}$. Therefore, these galaxies appear to be preferential located close to the critical density discussed above for the SFR-Density and T -R relations, *i.e.*, in the in-fall regions of C4 clusters. This is consistent with the observed decrease in the late spiral galaxies (Sc’s) witnessed in Figure 1.8.

In summary, the quality and quantity of the SDSS data allows us to study the environmental dependences of galaxy properties in greater detail than before. There does appear to be at least one critical density (at $\simeq 1h_7^2 \text{Mpc}^{-2}$) affecting the properties of galaxies and this could be due to the slow strangulation of star-formation in these spiral galaxies as they fall into denser environments.

R. C. Nichol

I would like to acknowledge the organizers of the conference for their invitation to participate and their hospitality in Pasadena. I also thank all my collaborators for allowing me to show their results and figures in this review. These include Chris Miller, Daniel Eisenstein, Risa Wechsler, Gus Evrard, Tim McKay, Tomo Goto, Michael Balogh, Ann Zabudloff, and my colleagues from both the SDSS–2dF LRG survey and SDSS. I thank Kathy Romer and Chris Miller for reading an earlier draft of this review.

Funding for the creation and distribution of the SDSS Archive has been provided by the Alfred P. Sloan Foundation, the Participating Institutions, the National Aeronautics and Space Administration, the National Science Foundation, the U.S. Department of Energy, the Japanese Monbukagakusho, and the Max Planck Society. The SDSS Web site is <http://www.sdss.org/>.

The SDSS is managed by the Astrophysical Research Consortium (ARC) for the Participating Institutions. The Participating Institutions are The University of Chicago, Fermilab, the Institute for Advanced Study, the Japan Participation Group, The Johns Hopkins University, Los Alamos National Laboratory, the Max-Planck-Institute for Astronomy (MPIA), the Max-Planck-Institute for Astrophysics (MPA), New Mexico State University, University of Pittsburgh, Princeton University, the United States Naval Observatory, and the University of Washington.

References

- Bahcall, N. A., et al., 2003, ApJ, submitted.
Balogh, M. L., Navarro, J. F., & Morris, S. L. 2000, ApJ, 540, 113
Beers, T. C., Flynn, K., & Gebhardt, K. 1990, AJ, 100, 32
Bekki, K., Shioya, Y., & Couch, W. J. 2002, ArXiv Astrophysics e-prints, 6207
Benson, A. J., Baugh, C. M., Cole, S., Frenk, C. S., & Lacey, C. G. 2000, MNRAS, 316, 107
Blanton, M. R. et al. 2001, AJ, 121, 2358
Blanton, M.R., Lupton, R.H., Maley, F.M., Young, N., Zehavi, I., Loveday, J. 2003, AJ, 125, 2276
Böhringer, H. et al. 2001, A&A, 369, 826
Bramel, D. A., Nichol, R. C., & Pope, A. C. 2000, ApJ, 533, 601
Bothun, G. D. & Sullivan, W. T. 1980, ApJ, 242, 903
Collins, C. A. et al. 2000, MNRAS, 319, 939
Couch, W. J., Barger, A. J., Smail, I., Ellis, R. S., & Sharples, R. M. 1998, ApJ, 497, 188
Diaferio, A., Kauffmann, G., Balogh, M. L., White, S. D. M., Schade, D., & Ellingson, E. 2001, MNRAS, 323, 999
Dressler, A. 1980, ApJ, 236, 351
Dressler, A. et al. 1997, ApJ, 490, 577
Eisenstein, D. J. et al. 2001, AJ, 122, 2267
Eisenstein, D. J. 2003, ApJ, 586, 718
Evrard, A. E. et al. 2002, ApJ, 573, 7
Fukugita, M., Ichikawa, T., Gunn, J. E., Doi, M., Shimasaku, K., & Schneider, D. P. 1996, AJ, 111, 1748
Gladders, M. D. & Yee, H. K. C. 2000, AJ, 120, 2148
Gómez, P. L. et al. 2003, ApJ, 584, 210
Goto, T. et al. 2002, AJ, 123, 1807
Goto, T. et al. 2003, ArXiv Astrophysics e-prints, 1303
Gunn, J. E. et al. 1998, AJ, 116, 3040
Guiderdoni, B. 1987, A&A, 172, 27
Hogg, D. W., Finkbeiner, D. P., Schlegel, D. J., & Gunn, J. E. 2001, AJ, 122, 2129
Hogg, D. W. et al. 2003, ApJL, 585, L5
Jenkins, A., Frenk, C. S., White, S. D. M., Colberg, J. M., Cole, S., Evrard, A. E., Couchman, H. M. P., & Yoshida, N. 2001, MNRAS, 321, 372

R. C. Nichol

- Kepner, J., Fan, X., Bahcall, N., Gunn, J., Lupton, R., & Xu, G. 1999, *ApJ*, 517, 78
- Kim, R. S. J. et al. 2002, *AJ*, 123, 20
- Kochanek, C. S., White, M., Huchra, J., Macri, L., Jarrett, T. H., Schneider, S. E., & Mader, J. 2003, *ApJ*, 585, 161
- Larson, R. B., Tinsley, B. M., & Caldwell, C. N. 1980, *ApJ*, 237, 692
- Lee, B., et al., 2003, *ApJ*, submitted.
- Lewis, I. et al. 2002, *MNRAS*, 334, 673
- Lucey, J. R. 1983, *MNRAS*, 204, 33
- Lupton, R. H., Gunn, J. E., Ivezić, Z., Knapp, G. R., Kent, S., & Yasuda, N. 2001, *ASP Conf. Ser.* 238: *Astronomical Data Analysis Software and Systems X*, 10, 269
- Miller, C. J. 2000, Ph.D. Thesis,
- Miller, C. J. et al. 2001, *AJ*, 122, 3492
- Nichol, R. C., Collins, C. A., Guzzo, L., & Lumsden, S. L. 1992, *MNRAS*, 255, 21P
- Nichol, R. C. et al. 2001, *Mining the Sky*, 613
- Nichol, R. C. 2002, *ASP Conf. Ser.* 268: *Tracing Cosmic Evolution with Galaxy Clusters*, 57
- Pier, J.R., Munn, J.A., Hindsley, R.B., Hennessy, G.S., Kent, S.M., Lupton, R.H., and Ivezić, Z. 2003, *AJ*, 125, 1559
- Peacock, J. A. & Nicholson, D. 1991, *MNRAS*, 253, 307
- Postman, M. & Geller, M. J. 1984, *ApJ*, 281, 95
- Postman, M., Huchra, J. P., & Geller, M. J. 1992, *ApJ*, 384, 404
- Postman, M., Lubin, L. M., Gunn, J. E., Oke, J. B., Hoessel, J. G., Schneider, D. P., & Christensen, J. A. 1996, *AJ*, 111, 615
- Postman, M. 2002, *ASP Conf. Ser.* 268: *Tracing Cosmic Evolution with Galaxy Clusters*, 3
- Schlegel, D. J., Finkbeiner, D. P., & Davis, M. 1998, *ApJ*, 500, 525
- Shimasaku, K. et al. 2001, *AJ*, 122, 1238
- Stoughton, C. et al. 2002, *AJ*, 123, 485
- Strauss, M. A. et al. 2002, *AJ*, 124, 1810
- Sutherland, W. 1988, *MNRAS*, 234, 159
- Treu, T., Ellis, R. S., Kneib, J. -, Dressler, A., Smail, I., Czoske, O., Oemler, A., & Natarajan, P. 2003, *ArXiv Astrophysics e-prints*, 3267
- van den Burgh, S. 1991, *PASP*, 103, 390
- York, D. G. et al. 2000, *AJ*, 120, 1579
- Zehavi, I. et al. 2002, *ApJ*, 571, 172